

# Application of dynamical eikonal approximation in elastic scattering reaction within 10-60 MeV/nucleon\*

Xiao-Yan Yun (韵小艳)<sup>1</sup> Dan-Yang Pang (庞丹阳)<sup>2</sup> Yi-Ping Xu (许祎萍)<sup>3†</sup>

<sup>1</sup>College of Physics and Optoelectronics, Taiyuan University of Technology, Taiyuan 030024, China

<sup>2</sup>School of Physics, Beihang University, Beijing 100191, China

<sup>3</sup>School of Nuclear Science and Engineering, North China Electric Power University, Beijing 102206, China

**Abstract:** Application of the dynamical eikonal approximation (DEA) to elastic scattering for Coulomb-dominated reactions at low energy is studied. Our test case consists of elastic scattering for  $^8\text{B}$ ,  $^9\text{C}$  and  $^{11}\text{Be}$  on  $^{208}\text{Pb}$  at 21.3, 25.2 and 12.7 MeV/nucleon, respectively. We introduce an empirical correction to the DEA method to account for Coulomb deflection, which significantly improves the description of elastic scattering of weakly-bound nuclei on heavy target. The angular distributions of elastic scattering obtained using the empirical correction show a good agreement with experimental data down to around 10 MeV/nucleon. Furthermore, we study the effect of relativistic kinematics corrections on the angular distributions of elastic scattering at incident energies between 20 and 60 MeV/nucleon. The results show that relativistic kinematics corrections are crucial for describing the angular distributions of elastic scattering as low as around 40 MeV/nucleon.

**Keywords:** elastic scattering, empirical correction, relativistic kinematics correction

**DOI:** CSTR:

## I. INTRODUCTION

With the development of radioactive ion beam physics in the mid-1980s, Isotope Separator On-Line (ISOL) facilities have been able to produce an increasing number of intermediate and high-energy beams, as well as short-lived nuclides. The number of observed nuclides has soared from approximately 300 to over 3000, while the number of theoretically predicted nuclides is estimated to be as high as 8000-10000, the vast majority of which are unstable. The study of exotic nuclei that lie far from the  $\beta$  stability line has emerged as one of the primary objectives in astrophysics. This research is intrinsically linked to the synthesis of elements and the evolution of celestial bodies following the Big Bang. Numerous novel phenomena have been uncovered in unstable nuclei. For example, the existence of neutron halo or neutron skin in some nuclei [1–3], the emergence of new magic numbers [4–7], and shape co-existence [8, 9], have been discovered. New phenomena continue to provide challenges to nuclear theory. These exotic nuclear structures also manifest themselves in reactions induced by radioactive nuclei. Elastic scattering induced by weakly-bound nuclei is of paramount importance, as it contains crucial information about the exotic structure and reaction mechanism of

these weakly-bound nuclei [10]. One particularly noticeable phenomenon is the significant reduction of the Coulomb-nuclear interference peak in the elastic scattering angular distributions of weakly-bound nuclei, such as  $^6\text{He}$  and  $^{11}\text{Be}$ . This reduction has been found to be caused by coupling effects from breakup reaction channels [11–16].

Several cutting-edge facilities, such as HIE-ISOLDE at CERN, are already operational or will soon provide radioactive ion beams (RIBs) at energies as low as 10 MeV/nucleon, necessitating robust theoretical support for experiments in this low-energy region. Recently, the High Intensity Heavy-ion Accelerator Facility (HIAF) has been established in Huizhou, Guang dong Province. This advanced facility can deliver high-intensity beams of both stable and radioactive ions, covering an extensive energy range from MeV/u to GeV/u. HIAF is expected to facilitate a wide array of elastic scattering experiments across this broad energy spectrum. Therefore, a reaction method applicable across a broad energy range, capable of effectively handling elastic scattering of weakly-bound nuclei, and featuring high numerical stability and computational efficiency is essential.

Some theories have been proposed to achieve this goal. Among them, the Continuum Discretized Coupled-Channels (CDCC) method has proven to be a highly suc-

Received 24 April 2025; Accepted 4 June 2025

\* Supported by the National Natural Science Foundation of China (Grants Nos. 12205098, U2067205) and the Fundamental Research Funds for the Central Universities(2025MS063)

† E-mail: xuy\_p\_sense@ncepu.edu.cn

©2025 Chinese Physical Society and the Institute of High Energy Physics of the Chinese Academy of Sciences and the Institute of Modern Physics of the Chinese Academy of Sciences and IOP Publishing Ltd. All rights, including for text and data mining, AI training, and similar technologies, are reserved.

successful tool for describing reactions induced by weakly-bound systems [17–20]. Since CDCC treats the collision in a fully quantum mechanical manner, it can be computationally demanding. Additionally, it faces challenges in achieving convergent results in the low energy region, while relativistic effects need to be considered in the high energy region [21].

Dynamical Eikonal Approximation (DEA) method relies on the eikonal approximation, which assumes that the projectile-target interaction occurs along a straight line [22, 23]. Based on this assumption, the wave function can be factorized into a plane wave multiplied by a function that varies smoothly with the projectile-target relative coordinate. This factorization allows us to perform reaction calculations more efficiently, reducing the computational time compared to the CDCC method. Moreover, the DEA method is an improvement over the traditional eikonal approximation, as it fully accounts for the dynamical effects of projectile excitation. This avoids the divergence issue in the integral over impact parameter  $b$  during cross section calculations within the eikonal approximation. In the previous studies, a detailed comparison between the CDCC and DEA methods for the breakup of the one-neutron halo nucleus  $^{15}\text{C}$  on  $^{208}\text{Pb}$  at an incident energy of 68 MeV/nucleon was conducted [24]. The results from both method are in excellent agreement. However, the DEA method fails to reproduce the CDCC results at 20 MeV/nucleon, as the eikonal approximation becomes invalid at such low energies, which stems from the Coulomb deflection. At low energies, significantly distorts the projectile-target relative motion from a pure plane wave. Therefore, it is crucial to try to find a way to correct it for low energy case in DEA. Recent results have shown that an empirical correction can markedly enhance the description of breakup reactions involving neutron-rich projectiles on heavy targets, down to incident energies of 20 MeV/nucleon [25]. The empirical correction replaces the impact parameter with the distance of closest approach of the corresponding classical trajectory. The excellent results obtained for neutron-rich nuclei, lead us to consider the extension of the correction to study the application of proton-rich nuclei. However, the feasibility of applying the DEA to the elastic scattering of proton-rich nuclei on heavy targets at these energies remains to be explored.

In this paper, our study examines three specific reactions:  $^8\text{B}$ ,  $^9\text{C}$  and  $^{11}\text{Be}$  impinging on  $^{208}\text{Pb}$  at incident energies of 21.3 MeV/nucleon, 25.2 MeV/nucleon, and 12.7 MeV/nucleon, respectively. We embark on the application of the DEA method to elastic scattering reactions at incident energies of several tens of MeV/nucleon with the empirical correction and relativistic kinematics correction. This energy range is typically considered to be one where relativistic effects are negligible. The study of this paper is to investigate the feasibility of extending the

DEA method to a wide energy range.

This paper is organized as follows: the theoretical framework of the dynamical eikonal approximation, empirical correction and relativistic kinematics correction are introduced in Section II; the results of empirical correction and relativistic kinematics correction with and without taking into account such corrections are shown in Section III; and the summary of this paper is given in Section IV.

## II. THEORETICAL FRAMEWORK

### A. Dynamical eikonal approximation

We consider a collision between a two-body projectile(P) and a structureless target(T) with mass  $m_T$  and charge  $Z_T e$ . The two-body projectile consists of a structureless core(c) with mass  $m_c$  and charge  $Z_c e$  and a fragment(f) with mass  $m_f$  and charge  $Z_f e$ . The projectile is described by an internal Hamiltonian  $H_0$

$$H_0 = -\frac{\hbar^2}{2\mu_{cf}} \Delta_r + V_{cf}(\mathbf{r}), \quad (1)$$

where  $\mu_{cf} = \frac{m_f m_c}{m_f + m_c}$  is the  $c$ - $f$  reduced mass of the projectile,  $\mathbf{r}$  is the relative coordinate of the fragment to the core.  $H_0$  is composed of the kinetic energy operator for the relative motion between core and fragment and of the core-fragment interaction potential  $V_{cf}$ . The potential  $V_{cf}$  contains an angular-momentum-dependent central term (including a Coulomb interaction) and a spin-orbit term involving the fragment spin, the spin of the core is neglected.

With this two-body description for the projectile, the P-T collision reduces to a three-body problem whose Hamiltonian( $H$ ) reads

$$H = \hat{T}_{PT} + H_0 + V_{cT} + V_{fT}, \quad (2)$$

where  $\hat{T}_{PT}$  is kinetic energy operator of projectile-target relative motion,  $V_{cT}$  and  $V_{fT}$  are the core-target and fragment-target systems interactions, respectively.

In order to study the reactions of projectile(P) on target(T), we need to solve the three-body Schrödinger equation

$$[\hat{T}_{PT} + H_0 + V_{cT} + V_{fT}] \Psi(\mathbf{R}_{PT}, \mathbf{r}) = E \Psi(\mathbf{R}_{PT}, \mathbf{r}), \quad (3)$$

where  $\Psi(\mathbf{R}_{PT}, \mathbf{r})$  is the three-body wave function.  $E$  is the total energy of the system,  $\mathbf{R}_{PT}$  is the coordinate of the projectile with respect to the target. In the DEA method, the resulting three-body Schrödinger equation is solved using the eikonal ansatz for the wave function

$$\Psi(\mathbf{R}_{PT}, \mathbf{r}) = e^{iKZ} \widehat{\Psi}(\mathbf{R}_{PT}, \mathbf{r}), \quad (4)$$

where  $K$  is wave number, which is related to the total energy  $E$ .

At high energies, one expects a weak dependence on  $\mathbf{R}_{PT}$  of  $\widehat{\Psi}$ . Using the factorization Eq.4 in Eq.3 and neglecting second-order derivatives of  $\widehat{\Psi}$  that are small at high velocities, we obtained

$$i\hbar v \frac{\partial}{\partial Z} \widehat{\Psi}(\mathbf{b}, Z, \mathbf{r}) = [(H_0 - E_0) + V_{cT} + V_{fT}] \widehat{\Psi}(\mathbf{b}, Z, \mathbf{r}), \quad (5)$$

where  $Z$  is the longitudinal components of  $\mathbf{R}_{PT}$ , the vector  $\mathbf{b} = (b, \phi)$  represents the transverse part of  $\mathbf{R}_{PT}$ .  $v$  is the relative velocity of projectile and target.  $E_0$  corresponds to projectile ground state of energy. In the standard eikonal implementation, the adiabatic approximation is performed to solve Eq.5. That approximation corresponds to neglecting the excitation energy of the projectile compared to the beam energy. In DEA, no such adiabatic approximation is made, and Eq.5 is solved numerically for each impact parameter  $\mathbf{b}$  imposing initial condition. Initially, the projectile is in its ground state  $n_0 l_0 j_0$  of energy  $E_0$  and has an initial P-T relative momentum  $\hbar K_0$ .  $j_0$  is the total angular momentum. It results from the coupling of the orbital angular momentum  $l_0$  and the spin of the fragment,  $m_0$  is its projection.  $\phi$  corresponds to the projectile ground state wave function.

$$\widehat{\Psi}^{(m_0)}(\mathbf{b}, t \rightarrow -\infty, \mathbf{r}) = \phi_{l_0 j_0 m_0}(E_0, \mathbf{r}), \quad (6)$$

where the variable  $t(Z = vt)$  is linked to the longitudinal part of  $\mathbf{R}_{PT}$ .

Let  $\widehat{\Psi}^{(m_0)}(\mathbf{b}, t, \mathbf{r})$  be a particular solution(to the particular orientation  $\mathbf{b}=(b, \phi=0)$ ) of Eq.5 corresponding to the initial condition  $\widehat{\Psi}^{(m_0)}(\mathbf{b}, t \rightarrow -\infty, \mathbf{r}) = \phi_{l_0 j_0 m_0}(\mathbf{r})$ .  $b$  is the impact parameter related to a classical trajectory. whereas in Eq.6  $\mathbf{b}$  is the transverse part of a quantal coordinate.

The elastic scattering differential cross section can be deduced from wave function(see Ref. [26] for more details).

$$\frac{d\sigma}{d\Omega_{el}} \propto \langle \phi_{l_0 j_0 m_0}(E_0, \mathbf{r}) | \widehat{\Psi}^{(m_0)}(\mathbf{R}, \mathbf{r}) \rangle, \quad (7)$$

## B. Empirical correction

As previously discussed, the DEA method is based on the eikonal approximation, which assumes that the interaction between the projectile and the target occurs along a straight line [22, 23]. However, in reality, the trajectory deviates from a straight line due to the deflection caused by the interaction with the target. At sufficiently high en-

ergies, the assumption of straight-line trajectories becomes more valid, as the deflection of the projectile by the target can be considered negligible. The eikonal approximation becomes invalid at low energies, which stems from the Coulomb deflection. At low energies, significantly distorts the projectile-target relative motion from a pure plane wave.

Fukui et al. discovered that the DEA no longer aligns with the CDCC calculation for the breakup of  $^{15}\text{C}$  on  $^{208}\text{Pb}$  at 20 MeV/nucleon. They observed that the discrepancies between DEA and CDCC are not only in the magnitude of the angular distributions but also in the angular distributions. Specifically, the oscillatory pattern of the DEA is shifted towards more forward angles compared to the CDCC calculation. To pinpoint the source of this discrepancy, they analyzed the contribution of each projectile-target relative angular momentum  $L$  to the total breakup cross section. They found that the DEA method tends to favor larger  $L$  values compared to the full CDCC calculation. To address this issue, they replaced the transverse component of the projectile-target relative coordinate  $b$  by the empirical value. For a collision dominated by the repulsive Coulomb interaction, that distance will be larger than  $b$ . The distance of closest approach  $b'$ , can be derived analytically [27, 28].

$$b' = \frac{\eta_0}{K_0} + \sqrt{\frac{\eta_0^2}{K_0^2} + b^2}, \quad (8)$$

where  $\eta$  is the Sommerfeld parameter,  $\eta_0 = \frac{Z_P Z_T e^2 \mu_{PT}}{\hbar^2 K_0}$ .  $Z_P$  and  $Z_T$  are the charge of the projectile and target, respectively.  $K_0$  is the wave number for the initial projectile-target, which is related to the total energy  $E = \hbar^2 K_0^2 / 2\mu_{PT} + E_0$ . Ref. [25] has shown that this simple empirical correction could improve significantly the description of breakup for neutron-rich nuclei on heavy targets at about 20 MeV/nucleon.

## C. Relativistic kinematics correction

For high-energy reactions that have transcended the nonrelativistic energy regime, the influence of relativistic effects can be taken into account. To provide a reliable theoretical interpretation of experimental data, it is imperative to develop a theoretical method of nuclear reactions that incorporates relativistic effects. This section introduces the relativistic kinematics corrections. When addressing relativity in nuclear reactions, several key aspects must be considered. For instance, the Schrödinger equation is not strictly valid in a relativistic context, and thus, at least, some re-interpolation of the nuclear optical potential is necessary [21]. Additionally, the parameters of reaction kinematics, including atomic masses and incident energies, require modification to account for re-

lativistic effects. The latter aspect is rather simple, but it has been found to be important for some cases. In this paper, we study the latter aspect. The velocity  $v$  of the projectile, which is utilized to solve the time-dependent Schrödinger equation (Eq.5), is calculated using the relativistic formula:

$$\frac{v}{c} = \sqrt{1 - \frac{1}{\left(1 + \frac{T_p}{m_p c^2}\right)^2}}, \quad (9)$$

where  $T_p$  is the initial kinetic energy of the projectile, and  $m_p$  is the mass of the projectile.

We also use the relativistic kinematics correction method proposed by Satchler [29]. Define  $\gamma_i^L$  as

$$\gamma_i^L = \frac{T_p^L}{m_p c^2} + 1, \quad (10)$$

where  $T_p^L$  is the incident energy per nucleon in the laboratory system.  $\gamma_p$  corresponds to the projectile:

$$\gamma_p = \frac{x_p + \gamma_i^L}{\sqrt{1 + x_p^2 + 2x_p \gamma_i^L}}, \quad (11)$$

and  $\gamma_T$  corresponds to the target nucleus:

$$\gamma_T = \frac{x_T + \gamma_i^L}{\sqrt{1 + x_T^2 + 2x_T \gamma_i^L}}, \quad (12)$$

where  $x_p = \frac{m_p c^2}{m_T c^2}$  and  $x_T = \frac{m_T c^2}{m_p c^2}$ . Then the masses of projectile nucleus and target nucleus after relativistic correction are  $m'_p = \gamma_p m_p$  and  $m'_T = \gamma_T m_T$ , and the reduced mass of the projectile-target system becomes:

$$\mu_{pT} = \frac{\frac{x_p + \gamma_i^L}{\sqrt{1 + x_p^2 + 2x_p \gamma_i^L}} m_p \frac{x_T + \gamma_i^L}{\sqrt{1 + x_T^2 + 2x_T \gamma_i^L}} m_T}{\frac{x_p + \gamma_i^L}{\sqrt{1 + x_p^2 + 2x_p \gamma_i^L}} m_p + \frac{x_T + \gamma_i^L}{\sqrt{1 + x_T^2 + 2x_T \gamma_i^L}} m_T}. \quad (13)$$

#### D. Inputs to the reaction method

We analyse the elastic scattering induced by  ${}^8\text{B}$ ,  ${}^9\text{C}$  and  ${}^{11}\text{Be}$  on  ${}^{208}\text{Pb}$  at 21.3, 25.2 and 12.7 MeV/nucleon, respectively. The nucleus  ${}^8\text{B}$  is usually considered as the archetypical one-proton halo nucleus, and methoded a valence proton and a  ${}^7\text{Be}$  core. The spectrum of  ${}^8\text{B}$  includes only one bound state with  $J^\pi = 2^+$ , which is obtained from the coupling of a  $0p_{3/2}$  proton with the  $\frac{3}{2}^-$  spin of the ground state of the  ${}^7\text{Be}$ . It is bound by a mere 137 keV in regard to the one-proton separation. In this

work, we use the version of description of  ${}^8\text{B}$  developed by Bertsch in Ref. [30].  ${}^9\text{C}$  is seen as a valence proton (in the  $0p_{3/2}$  orbital) and a  ${}^8\text{B}$  core. We use the version of description of  ${}^9\text{C}$  from Ref. [16].  ${}^{11}\text{Be}$  is seen as an inert  ${}^{10}\text{B}$  core in its  $0^+$  ground state, to which a neutron is bound by 0.5 MeV in the  $1s_{1/2}$  orbit. The  ${}^{11}\text{Be}$  description of this paper corresponds to a simplified version in Ref. [31, 32]. For computational reasons, we use a simple method of  ${}^8\text{B}$ ,  ${}^9\text{C}$  and  ${}^{11}\text{Be}$ , in which the spin and internal structure of the core are neglected.

The DEA equation is solved with the algorithm presented in Refs. [26, 33], the wave function is expanded over a mesh on the unit sphere containing  $N_\theta \times N_\phi$  points. We go up to  $10 \times 19$  points for these cases. The radial mesh is quasi-uniform, contains  $N_r = 800$  points, and extends up to  $r_{N_r} = 800$  fm. These calculations are performed for impact parameters  $b = 0-150$  fm with a discretization step that varies between 0.25 and 5 fm. As explained in Ref. [34], the angular distributions of elastic scattering are obtained with an extrapolation up to  $b_{max} = 800$  fm.

CDCC calculations were performed by the code FRESCO. Proton- ${}^7\text{Be}$  ( ${}^8\text{B}$ ) relative orbital angular momentum up to  $l_{max} = 3$  were included with all couplings up to multipolarity  $\lambda_{max} = 3$ . The continuum was discretized up to a maximum Proton- ${}^7\text{Be}$  relative energy of  $E_{max} = 15.3$  MeV, corresponding to  $k_{max} = 0.8$  fm $^{-1}$ , divided into eight equally spaced bins of width 0.1 fm $^{-1}$ , giving a total of 32 bins. The continuum states of the proton- ( ${}^9\text{C}$  case) system were discretized into nine bins up to a maximum excitation energy of  $E_{max} = 18.7$  MeV.  $k_{max} = 0.9$  fm $^{-1}$  were discretized into eight equally spaced bins of width 0.1 fm $^{-1}$ , giving a total of 36 bins. Proton- ${}^8\text{B}$  relative orbital angular momentum up to  $l_{max} = 3$  and  $\lambda_{max} = 3$  multipoles in the expansion of the coupling potentials. The continuum states of the neutron- ${}^{10}\text{Be}$  ( ${}^{11}\text{Be}$  case) system were discretized into nine bins up to a maximum excitation energy of  $E_{max} = 17.5$  MeV, corresponding to  $k_{max} = 0.9$  fm $^{-1}$ . The proton- ${}^8\text{B}$  relative orbital angular momentum up to  $l_{max} = 5$  were included with all couplings up to a maximum multipolarity  $\lambda_{max} = 5$ . Convergence of elastic scattering and breakup cross sections were ensured by with an increased model space.

In these calculations, the core-target interactions,  $V_{cT}$ , are obtained with the systematic single-folding method of nucleus-nucleus potentials [21], which accounts well for the nucleus-nucleus elastic scattering not only for stable nuclei but also for some unstable nuclei within the energy range of around 10-100 MeV/nucleon. The fragment-target interactions,  $V_{fT}$ , are taken from the CH89 systematics [35]. The Coulomb potentials for the  $c$ - $T$ ,  $f$ - $T$  and  $c$ - $f$  systems are calculated with a uniform distribution of a charge sphere with a radius  $R_c = r_c(A_T^{1/3} + A_c^{1/3})$ ,  $r_c(A_T^{1/3})$ , and  $r_c(A_c^{1/3})$ , respectively, where  $r_c = 1.25$  fm, and  $A_T$  and  $A_c$  are the mass numbers of the target and the

core nuclei, respectively.

### III. RESULTS AND DISCUSSIONS

Figs. 1 and 2 show the analysis of  $^8\text{B}$  and  $^9\text{C}$  on  $^{208}\text{Pb}$  at low energies (21.3 and 25.2 MeV/nucleon, respectively). These figures display the angular distributions of elastic scattering (ratio to Rutherford,  $\sigma/\sigma_R$ ) as a function of the center of mass of scattering angles,  $\theta_{c.m.}$ . The pink dotted curves represent the results of DEA method with empirical correction (labeled with "Corr"), while the green dash-dotted curves correspond to the results of DEA method without empirical correction (labeled with "NoCorr"). The blue dashed curves correspond to the results of the CDCC method. As seen in Fig. 1, the results of the CDCC and experimental data agree very well with each other. The results of the DEA (labeled with

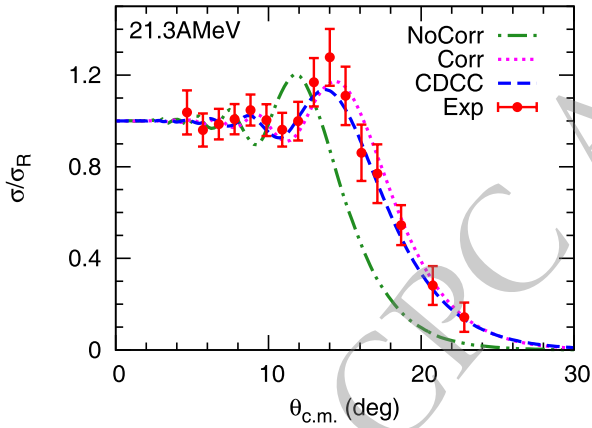


**Fig. 1.** (Color online) Comparisons between theoretical and experimental (red circle) angular distributions for the elastic scattering of  $^8\text{B}$  on  $^{208}\text{Pb}$  at 21.3 MeV/nucleon (see text for details). The experimental data is from Ref. [36].

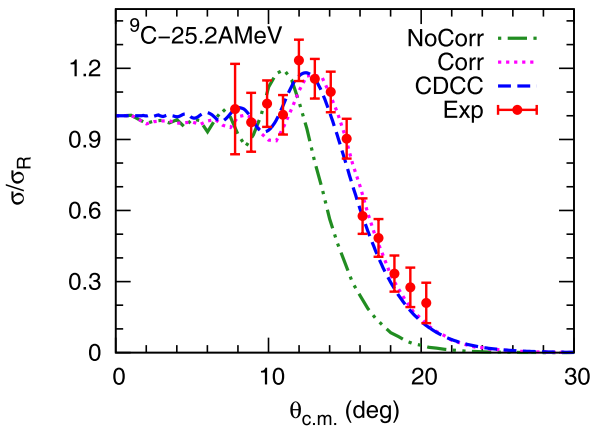


**Fig. 2.** (Color online) Comparisons between theoretical and experimental (red circle) angular distributions for the elastic scattering of  $^9\text{C}$  on  $^{208}\text{Pb}$  at 25.2 MeV/nucleon (see text for details). The experimental data is from Ref. [16].

"NoCorr") and experimental data no longer agree with each other at 21.3 MeV/nucleon. We see that not only do the DEA and CDCC differ in magnitude, but also DEA oscillatory pattern is shifted to forward angle compared to the CDCC. When the empirical correction is switched on, the agreement between the two methods is good. The results confirm that the empirical correction is very effective. It improves significantly the agreement with CDCC method. The results in Fig. 2 are very similar to those observed in Fig. 1 for  $^8\text{B}$ . Note that the result of DEA using the correction seems to have a good agreement with CDCC and experimental data.

To further verify the applicability of the empirical correction to lower energy reaction, we study the case of  $^{11}\text{Be}$  on a lead target at 12.7 MeV/nucleon. As seen in Fig. 3, compared to the case at around 20 MeV/nucleon, the discrepancy between the results of the DEA and the CDCC becomes more pronounced at 12.7 MeV/nucleon. Nevertheless, the DEA still successfully reproduces the angular distributions obtained from the CDCC. The results of these calculation suggest that DEA could be extended its range of validity down to 10 MeV/nucleon in Coulomb-dominated collisions.

The difference observed between the DEA (labeled with "NoCorr") and experimental data at low energy is related to the root: the lack of Coulomb deflection in the DEA. Based on the eikonal approximation, the DEA presumes that the incoming plane-wave motion of the projectile remains largely unperturbed by its interaction with the target. Nevertheless, the results show that the lack of Coulomb deflection for the DEA calculations can be efficiently corrected by the empirical correction (see the curve labeled with "Corr"). Albeit efficient, the empirical correction is not perfect. A slight shift of the oscillatory pattern to the larger scattering angles can be seen compared to the experimental data. However, its oscillatory

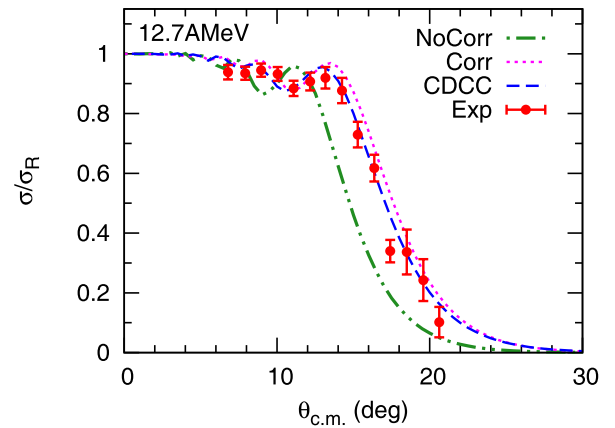


**Fig. 3.** (Color online) Comparisons between theoretical and experimental (red circle) angular distributions for the elastic scattering of  $^{11}\text{Be}$  on  $^{208}\text{Pb}$  at 12.7 MeV/nucleon (see text for details). The experimental data is from Ref. [15].

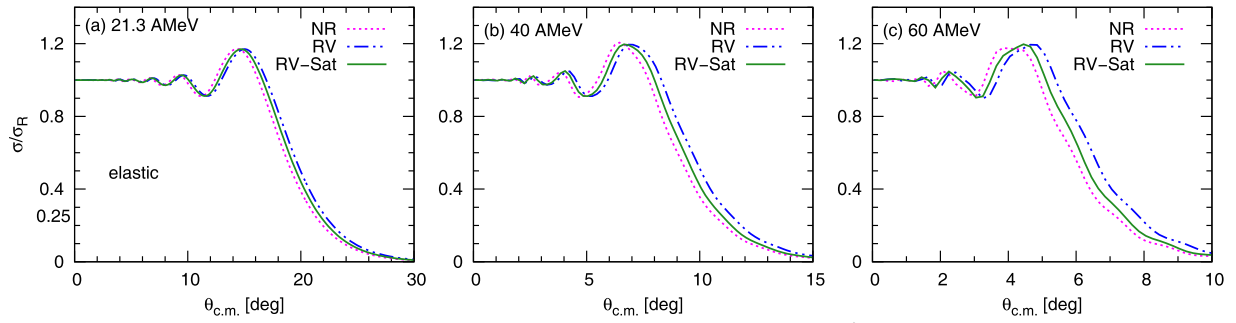


**Fig. 4.** (color online) Effect of the relativistic corrections on angular distributions of elastic scattering for  ${}^8\text{B}$  on  ${}^{208}\text{Pb}$  at different incident energies. The dotted, dashed-double-dotted and solid curves, labeled with "NR", "RV" and "RV-Sat", respectively, correspond to results without taking into account the relativistic corrections, taking into account the relativistic correction of the velocity and taking into account velocity's and Satchler's relativistic correction.

pattern is now in phase with experimental data. This correction provides a simple and effective way to account for Coulomb deflection in the DEA method. In the following calculations, the empirical correction is included.

The calculations in Figs. 1, 2 and 3 are performed within the nonrelativistic framework. However, it is well-known that at sufficiently high incident energies, relativistic effects have to be taken into account. We investigate reactions with incident energies in the range of several tens of MeV per nucleon. At these energy levels, relativistic effects may start to become significant. Consequently, we incorporate relativistic kinematics corrections into the subsequent calculations to account for this influence.

In order to study how the importance of the relativistic corrections evolves with the incident energy of the projectile, we study the elastic scattering reaction of  ${}^8\text{B}$  on  ${}^{208}\text{Pb}$  at 20, 40, 60 MeV/nucleon. The results are shown in Fig. 4. The pink dotted curves represent the results obtained without considering relativistic corrections. The blue dashed-double-dotted curves represent the results with the inclusion of the relativistic correction for velocity (Eq. 9), marked as "RV". The green curves correspond to the results incorporating both velocity's and Satchler's relativistic corrections, labeled as "RV-Sat". As expected, the effect of relativistic corrections is minimal at lower incident energies. It is evident that the significance of relativistic corrections becomes apparent at 40 MeV/nucleon and increases with higher incident energies.

#### IV. SUMMARY

In this study, we study the application of the Dynam-

ical Eikonal Approximation (DEA) method for a wide energy range. We study the angular distributions of elastic scattering of  ${}^8\text{B}$ ,  ${}^9\text{C}$ , and  ${}^{11}\text{Be}$  on  ${}^{208}\text{Pb}$  at incident energies between around 10 to 60 MeV/nucleon. We compare the continuum discretized coupled channel (CDCC) method and DEA method for the angular distributions of elastic scattering. Our results show that the difficulty to properly describe the elastic scattering for low energy case within the DEA method. However, we find that an empirical correction significantly enhances the methods ability to reproduce the Coulomb deflection, which was previously identified as a missing component in the DEA. With this correction, the agreement between the DEA results and those from the CDCC method is markedly improved. Moreover, the DEA using the empirical correction also shows a good agreement with experimental data. We also study the effect of relativistic kinematics corrections on the angular distributions of elastic scattering for  ${}^8\text{B}$  on  ${}^{208}\text{Pb}$  at incident energies ranging from 20 to 60 MeV/nucleon. We examine the effects of relativistic corrections on these angular distributions. Our calculations reveal that relativistic corrections play a crucial role in accurately describing the angular distributions of elastic scattering, even at relatively low incident energies of around 40 MeV/nucleon. From these results, we conclude that DEA method including the empirical correction and relativistic corrections can provide an efficient alternative tool to describe the elastic scattering of weakly-bound within a wide energy region. In order to extend the DEA method to the high regions of incident energies up to around 1 GeV/nucleon, a suitable phenomenological potential for reactions in the high energy region is important. We plan to study this in future work.

#### References

- [1] I. Tanihata, H. Hamagaki, O. Hashimoto, Y. Shida, N. Yoshikawa, K. Sugimoto, O. Yamakawa, T. Kobayashi, and N. Takahashi, *Phys. Rev. Lett.* **55**, 2676 (1985)
- [2] A. S. Jensen, K. Riisager, D. V. Fedorov, and E. Garrido, *Rev. Mod. Phys.* **76**, 215 (2004)
- [3] R. Kanungo, W. Horiuchi, G. Hagen, G. R. Jansen, P. Navratil, F. Ameil, J. Atkinson, Y. Ayyad, D. Cortina-Gil, I. Dillmann, A. Estradé, A. Evdokimov, F. Farinon, H.

- Geissel, G. Guastalla, R. Janik, M. Kimura, R. Knöbel, J. Kurcewicz, Yu. A. Litvinov, M. Marta, M. Mostazo, I. Mukha, C. Nociforo, H. J. Ong, S. Pietri, A. Prochazka, C. Scheidenberger, B. Sitar, P. Strmen, Y. Suzuki, M. Takechi, J. Tanaka, I. Tanihata, S. Terashima, J. Vargas, H. Weick, and J. S. Winfield, *Phys. Rev. Lett.* **117**, 102501 (2016)
- [4] A. Ozawa, T. Kobayashi, T. Suzuki, K. Yoshida, and I. Tanihata, *Phys. Rev. Lett.* **84**, 5493 (2000)
- [5] R. Kanungo, C. Nociforo, A. Prochazka, T. Aumann, D. Boutin, D. Cortina-Gil, B. Davids, M. Diakaki, F. Farion, H. Geissel, R. Gernhäuser, J. Gerl, R. Janik, B. Jonson, B. Kindler, R. Knöbel, R. Krücken, M. Lantz, H. Lenske, Y. Litvinov, B. Lommel, K. Mahata, P. Maierbeck, A. Musumarra, T. Nilsson, T. Otsuka, C. Perro, C. Scheidenberger, B. Sitar, P. Strmen, B. Sun, I. Szarka, I. Tanihata, Y. Utsuno, H. Weick, and M. Winkler, *Phys. Rev. Lett.* **102**, 152501 (2009)
- [6] D. Steppenbeck, S. Takeuchi, N. Aoi, P. Doornenbal, M. Matsushita, H. Wang, H. Baba, N. Fukuda, S. Go, M. Honma, J. Lee, K. Matsui, S. Michimasa, T. Motobayashi, D. Nishimura, T. Otsuka, H. Sakurai, Y. Shiga, P.-A. Soderstrom, T. Sumikama, H. Suzuki, R. Taniuchi, Y. Utsuno, J. J. Valiente-Dobon, and K. Yoneda, *Nature* **502**, 207 (2013)
- [7] M. Rosenbusch, P. Ascher, D. Atanasov, C. Barbieri, D. Beck, K. Blaum, Ch. Borgmann, M. Breitenfeldt, R. B. Cakirli, A. Cipollone, S. George, F. Herfurth, M. Kowalska, S. Kreim, D. Lunney, V. Manea, P. Navrátil, D. Neidherr, L. Schweikhard, V. Somà, J. Stanja, F. Wienholtz, R. N. Wolf, and K. Zuber, *Phys. Rev. Lett.* **114**, 202501 (2015)
- [8] Kris Heyde and John L. Wood, *Rev. Mod. Phys.* **83**, 1467 (2011)
- [9] X. F. Yang, C. Wraith, L. Xie, C. Babcock, J. Billowes, M. L. Bissell, K. Blaum, B. Cheal, K. T. Flanagan, R. F. Garcia Ruiz, W. Gins, C. Gorges, L. K. Grob, H. Heylen, S. Kaufmann, M. Kowalska, J. Kraemer, S. Malbrunot-Ettenauer, R. Neugart, G. Neyens, W. Nörtershäuser, J. Papuga, R. Sánchez, and D. T. Yordanov, *Phys. Rev. Lett.* **116**, 182502 (2016)
- [10] J. J. Kolata, V. Guimarães, and E. F. Aguilera, *The European Physical Journal A* **52**, 123 (2016)
- [11] O.R. Kakuee, M.A.G. Alvarez, M.V. Andrés, S. Cherubini, T. Davinson, A. Di Pietro, W. Galster, J. Gómez-Camacho, A.M. Laird, M. Laméhi-Rachti, I. Martel, A.M. Moro, J. Rahighi, A.M. Sánchez-Benitez, A.C. Shotton, W.B. Smith, J. Vervier, and P.J. Woods, *Nuclear Physics A* **765**(3), 294 (2006)
- [12] K. Rusek, N. Keeley, K. W. Kemper, and R. Raabe, *Phys. Rev. C* **67**, 041604 (2003)
- [13] A.M. Sánchez-Benitez, D. Escrig, M.A.G. Álvarez, M.V. Andrés, C. Angulo, M.J.G. Borge, J. Cabrera, S. Cherubini, P. Demaret, J.M. Espino, P. Figuera, M. Freer, J.E. García-Ramos, J. Gómez-Camacho, M. Gulino, O.R. Kakuee, I. Martel, C. Metelko, A.M. Moro, F. Pérez-Bernal, J. Rahighi, K. Rusek, D. Smirnov, O. Tengblad, P. Van Duppen, and V. Ziman, *Nuclear Physics A* **803**(1), 30 (2008)
- [14] Y. Y. Yang, X. Liu, and D. Y. Pang, *Phys. Rev. C* **94**, 034614 (2016)
- [15] F.F. Duan, Y.Y. Yang, K. Wang, A.M. Moro, V. Guimarães, D.Y. Pang, J.S. Wang, Z.Y. Sun, Jin Lei, A. Di Pietro, X. Liu, G. Yang, J.B. Ma, P. Ma, S.W. Xu, Z. Bai, X.X. Sun, Q. Hu, J.L. Lou, X.X. Xu, H.X. Li, S.Y. Jin, H.J. Ong, Q. Liu, J.S. Yao, H.K. Qi, C.J. Lin, H.M. Jia, N.R. Ma, L.J. Sun, D.X. Wang, Y.H. Zhang, X.H. Zhou, Z.G. Hu, and H.S. Xu, *Physics Letters B* **811**, 135942 (2020)
- [16] Y. Y. Yang, X. Liu, D. Y. Pang, D. Patel, R. F. Chen, J. S. Wang, P. Ma, J. B. Ma, S. L. Jin, Z. Bai, V. Guimarães, Q. Wang, W. H. Ma, F. F. Duan, Z. H. Gao, Y. C. Yu, Z. Y. Sun, Z. G. Hu, S. W. Xu, S. T. Wang, D. Yan, Y. Zhou, Y. H. Zhang, X. H. Zhou, H. S. Xu, G. Q. Xiao, and W. L. Zhan, *Phys. Rev. C* **98**, 044608 (2018)
- [17] N. Austern, Y. Iseri, M. Kamimura, M. Kawai, G. Rawitscher, and M. Yahiro, *Physics Reports* **154**(3), 125 (1987)
- [18] J. A. Tostevin, F. M. Nunes, and I. J. Thompson, *Phys. Rev. C* **63**, 024617 (2001)
- [19] M. Avrigeanu and A. M. Moro, *Phys. Rev. C* **82**, 037601 (2010)
- [20] Y. Kucuk and A. M. Moro, *Phys. Rev. C* **86**, 034601 (2012)
- [21] Y. P. Xu and D. Y. Pang, *Phys. Rev. C* **87**, 044605 (2013)
- [22] R. J. Glauber. volume 1, page 315. Interscience, New York, 1959.
- [23] K. Yabana Y. Suzuki, R. G. Lovas and K. Varga. page 315.
- [24] P. Capel, H. Esbensen, and F. M. Nunes, *Phys. Rev. C* **85**, 044604 (2012)
- [25] T. Fukui, K. Ogata, and P. Capel, *Phys. Rev. C* **90**, 034617 (2014)
- [26] G. Goldstein, D. Baye, and P. Capel, *Phys. Rev. C* **73**, 024602 (2006)
- [27] C. A. Bertulani and P. Danielewicz. page 515. Bristol, England, 2004.
- [28] C.A. Bertulani, C.M. Campbell, and T. Glasmacher, *Computer Physics Communications* **152**(3), 317 (2003)
- [29] W.J. Satchler G R. R.L. Varner, *Nucl. Phys. A* **540**(1), 533 (1992)
- [30] H. Esbensen and G. F. Bertsch, *Nuclear Physics A* **600**(1), 37 (1996)
- [31] P. Capel, R. C. Johnson, and F. Nunes, *Phys. Lett. B* **705** (2011)
- [32] P. Capel, R. C. Johnson, and F. M. Nunes, *Phys. Rev. C* **88**, 044602 (2013)
- [33] P. Capel, D. Baye, and V. S. Melezhik, *Phys. Rev. C* **68**, 014612 (2003)
- [34] X Y Yun, F Colomer, D Y Pang, and P Capel, *Journal of Physics G: Nuclear and Particle Physics* **46**(10), 105111 (2019)
- [35] R.L. Varner, W.J. Thompson, T.L. McAbee, E.J. Ludwig, and T.B. Clegg, *Phys. Rep.* **201**(2), 57 (1991)
- [36] Y. Y. Yang, J. S. Wang, Q. Wang, D.Y. Pang, J. B. Ma, M. R. Huang, J. L. Han, P. Ma, S. L. Jin, Z. Bai, Q. Hu, L. Jin, J. B. Chen, N. Keeley, K. Rusek, R. Wada, S. Mukherjee, Z. Y. Sun, R. F. Chen, X. Y. Zhang, Z. G. Hu, X. H. Yuan, X. G. Cao, Z. G. Xu, S. W. Xu, C. Zhen, Z. Q. Chen, Z. Chen, S. Z. Chen, C. M. Du, L. M. Duan, F. Fu, B. X. Gou, J. Hu, J. J. He, X. G. Lei, S. L. Li, Y. Li, Q. Y. Lin, L. X. Liu, F. D. Shi, S. W. Tang, G. Xu, X. Xu, L. Y. Zhang, X. H. Zhang, W. Zhang, M. H. Zhao, Z. Y. Guo, Y. H. Zhang, H. S. Xu, and G. Q., *Phys. Rev. C* **87**, 044613 (2013)